Effect of screening on the relaxation dynamics in a Coulomb glass

Preeti Bhandari [1], Vikas Malik [2,*] and Moshe Schechter [1]
[1]*Department of Physics, Ben-Gurion University of the Negev, Beer Sheva 84105, Israel*
[2]*Department of Physics and Material Science, Jaypee Institute of Information Technology, Uttar Pradesh 201309, India*

(Received 13 June 2023; revised 2 September 2023; accepted 11 September 2023; published 19 September 2023)

This paper examines the relaxation dynamics of a two-dimensional Coulomb glass lattice model with high disorder. The study aims to investigate the effects of disorder and Coulomb interactions on glassy dynamics by computing the eigenvalue distribution of the linear dynamical matrix using the mean-field approximation. The findings highlight the significance of the single-particle density of states (DOS) as the main controlling parameter affecting the relaxation at intermediate and long times. For the model with unscreened Coulomb interactions, our results indicate that the depletion of the DOS near the Fermi level leads to logarithmic decay at intermediate times. As the relaxation progresses to longer times, a power-law decay emerges, with the exponent approaching zero as the disorder strength increases, suggesting the manifestation of logarithmic decay at high disorders. The effects of screening of interactions on the dynamics are also studied at various screening and disorder strengths. The findings reveal that screening leads to the filling of the gap in the density of states, causing deviation from logarithmic decay at intermediate disorders. Moreover, in the strong disorder regime, the relaxation dynamics are dominated by disorder, and even with screened Coulomb interactions, the electronic relaxation remains similar to the unscreened case. The time at which crossover to exponential decay occurs increases with increasing disorder and interaction strength.

DOI: 10.1103/PhysRevB.108.094208

I. INTRODUCTION

Slow dynamics is one of the most striking features of glasses, as observed both numerically [1–4] and experimentally [5–14]. Understanding the origin of these slow dynamics is an important problem in condensed-matter physics. In disordered electronic systems, it is generally believed that the interplay of disorder and unscreened Coulomb interaction results in glassy behavior. The Coulomb glass (CG) model, which exhibits many characteristics of glass [4, 15–26], provides an excellent framework for understanding these phenomena. The CG model describes a disordered lattice of electrons that interact via unscreened Coulomb interactions. The strength of disorder and interaction between the electrons plays an important role in the formation of the soft Coulomb gap at high disorders [27–37]. The gap in the single-particle density of states (DOS) of the system is filled up as the temperature is increased [38], or if the electron-electron interaction is screened. Since unscreened Coulomb interactions are pivotal to the formation of the soft Coulomb gap at high disorder, one concludes that the slow relaxation is due to the interplay between disorder and interactions. This has been observed experimentally [39–47] for samples where both disorder and interactions are strong, but the question remains about the role of long-range Coulomb interactions played in slow relaxation.

The relaxation dynamics in a CG system can be studied experimentally in a variety of procedures, for example, quenching the system from high temperatures to low temperatures [48]. In this case one observes that the excess conductance of the sample initially relaxes very fast, followed by a slow relaxation. Similarly, a nonequilibrium state can also be created using gate protocols [7,49] or by absorption of light [50,51]. In all cases, the slow relaxation behavior can be explained by the formation of the Coulomb gap in the density of states (DOS) [52–54]. The gap forms slowly with time, and its width depends on the strength of the disorder and the electron-electron interactions.

Experiments [55] have also been carried out on samples having screened Coulomb interactions, in which a metallic plate is employed to screen the interaction between electrons. The sluggish dynamics seen in these samples are surprisingly quite similar to those in the reference sample without the metallic plate.

In this paper we investigate the role of screening on slow dynamics in the CG model using mean-field approximation. We compare the dynamics with unscreened Coulomb interactions to the dynamics with screened Coulomb interactions as a function of disorder strength. Our aim is to gain a better understanding of the interplay between disorder and interactions and the role of screening on slow dynamics. Other effects of the screening not considered here, such as the polaronic effect [56], may affect the dynamics.

Our paper is organized as follows. In Sec. I we describe the experimental setup. In Secs. I and II we discuss the experimental setup and the model Hamiltonian. In Sec. IV A we present the results of the single-particle density of states. In Sec. IV B we discuss the relaxation dynamics in the presence of unscreened Coulomb interactions and also in the case of

*vikasm76@gmail.com

screened Coulomb interactions. Finally, in Sec. V we conclude the paper with a summary of our results.

II. EXPERIMENTAL SETUP

Anderson insulators that possess strong disorder and strong interaction (high carrier concentration) demonstrate slow relaxation and memory effects. The precise influence of the long-range unscreened Coulomb interactions on these phenomena occurring outside of equilibrium is not yet well understood. Recently, experiments [55] were conducted to investigate the relaxation of In_xO samples. This was achieved by introducing a metallic gold plate in close proximity to the sample, with the sample being situated between two layers of SiO_2. The gold film was deposited on one of the SiO_2 layers. The spacing between the screening layer (gold film) and the sample was controlled by altering the thickness (d) of the SiO_2 layer. The degree of screening decreases as the SiO_2 layer thickness increases. The concentration of carriers was deliberately maintained at relatively low levels, resulting in shorter relaxation times of the order of 10^3 s. These short relaxation times allowed an examination of deviations from the expected logarithmic relaxation law by comparing the outcomes of the screened and unscreened (reference) samples.

III. MODEL

The Hamiltonian used in this paper has been defined in terms of occupation numbers n_i and the on-site random field energy ϕ_i. In dimensionless units, the Hamiltonian at half-filling is given by

$$\mathcal{H}\{n_i\} = \sum_{i=1}^{N} \phi_i n_i + \frac{1}{2}\sum_{i\neq k} J_{ik}(n_i - 1/2)(n_k - 1/2). \quad (1)$$

The occupation number n_i takes on values 0 or 1, corresponding to the absence or presence of an electron at site i, and ϕ_i is the random on-site energy. The interaction between sites i and k is given by J_{ik}, which can be either unscreened Coulomb interaction (CI) [57–60] or screened Coulomb interaction (SI) [61]:

$$J_{ik} = \frac{1}{r_{ik}}, \quad \text{unscreened Coulomb interaction} \quad (2a)$$

$$J_{ik} = \frac{1}{r_{ik}} - \frac{1}{\sqrt{r_{ik}^2 + 4d^2}}, \text{ screened interaction,} \quad (2b)$$

where r_{ik} is the distance between sites i and k under periodic boundary conditions, and d is the separation between the metallic plate and the system (we call it the screening distance here).

IV. RESULTS

A. Local equilibrium

The first step in calculating the relaxation dynamics is to find the local equilibrium state at a finite temperature for a given disorder realization. We use the mean-field (MF) approximation to calculate the average occupancy at each site i at temperature $T = \beta^{-1}$. The average occupation is given by

$$F_i = f_{FD}(\varepsilon_i) = 1/(\exp[\beta\varepsilon_i] + 1), \quad (3)$$

where f_{FD} is the Fermi-Dirac distribution function, and ε_i is the Hartree energy at site i, defined using a self-consistent equation as

$$\varepsilon_i = \phi_i + \sum_{k\neq i} J_{ik}(F_k - 1/2). \quad (4)$$

We solve the self-consistent equations for a square lattice with $N = 1600$ sites under periodic boundary conditions. The values of ϕ_i are drawn from a box distribution of width $[-W/2, W/2]$, where W is the disorder strength. To ensure the accuracy of our results, we average over 500 random configurations.

We perform our calculations for both cases of unscreened and screened Coulomb interactions to allow investigation of the influence of screening on the dynamics of the system. The screened interaction takes into account the electron-electron Coulomb interaction and their images in the metal plane that is parallel to the system at a distance d (screening distance). As the distance between the metallic plate and the system increases, the screening of electron-electron interaction decreases. The comparison between the density of states (DOS) with screened and unscreened interactions is shown in Fig. 1(a). In the presence of unscreened Coulomb interactions and at finite temperatures, the density of states (DOS) is expected to have a soft gap near the Fermi level (μ) such that $g(\mu) \propto T^{D-1}$, where D is the dimension [28,62]. As a consequence, the minimum DOS value within the Coulomb gap is attained at the Fermi level and is the main characteristic defining the Coulomb gap. It is noteworthy that alternative methodologies for DOS computation [31,32,35,38,63,64] reveal that the temperature-induced filling of the gap is comparatively subdued within the context of mean-field approximations. The screening of Coulomb interactions leads to the filling of the gap.

To quantify the effect of disorder and screening on the smearing of the gap, we look into the DOS at the Fermi level ($g(\mu)$) as a function of d at different disorder strengths (W), as shown in Fig. 1(b). We also calculate the relative change in $g(\mu)$, which is defined as

$$\Delta g(\mu) = \frac{g(\mu)_{SI} - g(\mu)_{CI}}{\delta_g}. \quad (5)$$

Here $g(\mu)_{SI}$ is the DOS at the Fermi level due to screened interactions, $g(\mu)_{CI}$ is the DOS at the Fermi level due to Coulomb interactions, and $\delta_g \approx W^{-1}$ is the height of the DOS in the case of unscreened Coulomb interactions [see Fig. 1(a) for details].

B. Relaxation dynamics

The conventional explanation for the sluggish dynamics in glasses is that the system struggles to overcome potential barriers and gets trapped in metastable states. This approach focuses on the energy landscape with multiple valleys [45,62]. In contrast, the present paper considers a single valley scenario where the system is only slightly off its local equilibrium [26,65]. The relaxation dynamics of the system back to

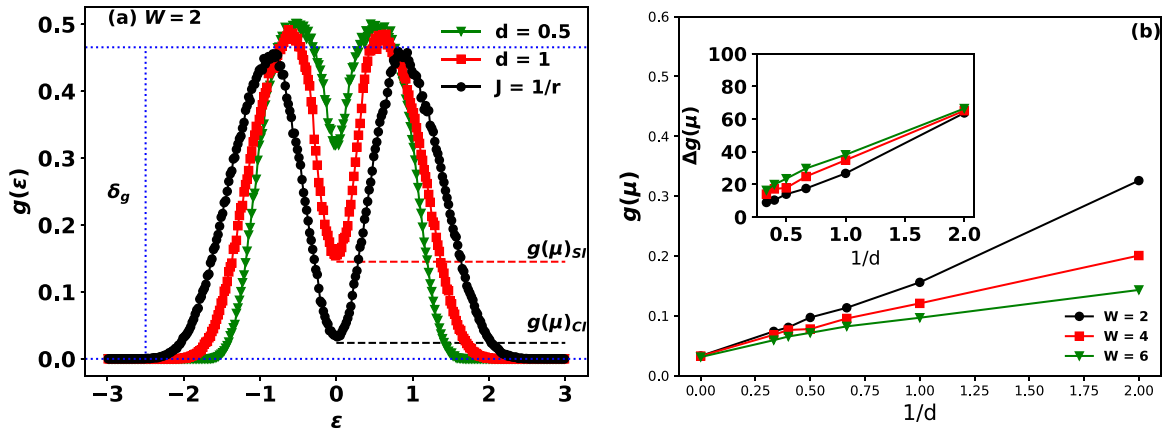

FIG. 1. (a) Histogram of the Hartree energy ε [obtained using Eq. (4)] at $W = 2$ and $\beta = 10$. Here $J = 1/r$ corresponds to the Coulomb interaction case as defined in Eq. (2a), and $d = 1$ and $d = 0.5$ correspond to the screened interaction case [see Eq. (2b)]. δ_g is the height of the density of states (DOS) in the unscreened Coulomb interaction case. $g(\mu)_{SI}$ and $g(\mu)_{CI}$ are the DOS at the Fermi level ($\mu = \varepsilon = 0$) for the screened and unscreened case, respectively. (b) The density of states at the Fermi level $g(\mu)$ as a function of distance d. Inset shows the relative change in $g(\mu)$, which is calculated using Eq. (5).

its local equilibrium state are then observed using a generalized master equation [66]:

$$\frac{d}{dt}P(\{n_\mu\},t) = -\sum_{\mu\neq\nu} W_{\mu\to\nu}\;\; P(\{n_\mu\},t) + \sum_{\nu\neq\mu} W_{\nu\to\mu}\;\; P(\{n_\nu\},t)\,, \tag{6}$$

where $W_{\mu\to\nu}$ signifies the transition rates from state μ to ν, and $P(\{n_\mu\},t)$ is the likelihood that the system will be in state μ at the time t. Single-electron transfer or multiple-electron transfer can be used to describe the transition rates that conserve the particle (electron) number. In this paper we study the evolution by considering only the single electron transitions. The effect of multiparticle hops is not considered here.

When using the MF approximation, close to local equilibrium, the average occupation at site i can be given as

$$N_i(t) = f_i + \delta N_i, \tag{7}$$

where f_i is the occupancy at local stable point, $f_i = m_i - 1/2$, and δN_i is the deviation of average occupancy from f_i. The time evolution of the fluctuation is controlled by the matrix equation

$$\frac{d}{dt}\delta N_i = -\sum_l A_{il}\;\; \delta N_l, \tag{8}$$

where we define

$$\Gamma_{ik} = \frac{1}{2\tau}\gamma(r_{ik})\;\; f_i(1-f_k)\;\; f_{FD}\big(\varepsilon_k^e - \varepsilon_i^e\big), \tag{9a}$$

$$\Gamma_{ki} = \frac{1}{2\tau}\gamma(r_{ki})\;\; f_k(1-f_i)\;\; f_{FD}\big(\varepsilon_i^e - \varepsilon_k^e\big), \tag{9b}$$

$$A_{ii} = \sum_{k\neq i}\frac{\Gamma_{ik}}{f_i(1-f_i)}, \tag{9c}$$

$$A_{il} = -\frac{\Gamma_{li}}{f_l(1-f_l)} - \frac{1}{T}\sum_{k(\neq l\neq i)}\Gamma_{ik}\;\;(J_{kl}-J_{il}). \tag{9d}$$

Here $\gamma(r_{ik}) = \gamma_0 e^{-r_{ik}}/\xi$, where $\gamma_0 \approx 10^{12}\,\mathrm{s}^{-1}$ is a constant, and ξ is the localization length. $f_{FD}(\varepsilon) = 1/(\exp[\varepsilon/T]+1)$ is the Fermi-Dirac distribution, and ε_k^e represents the Hartree energy of site k in equilibrium. The equilibrium electron transition rate from site i to k (k to i) is given by Γ_{ik} (Γ_{ki}) and $\Gamma_{ik} = \Gamma_{ki}$. In the context of our work, when we refer to the energy of the system, we are specifically referring to the energy of electrons, which is given by Eq. (1) (electron-phonon interaction is neglected). Within the framework of mean-field approximation, the change in energy of electrons due to an electron transition from site i to site k is captured by $\varepsilon_k - \varepsilon_i$, where ε_k and ε_i represent the single-particle energy (Hartree energies) at sites k and i, respectively. It is important to note that the actual energy change during the transition from the site i to k is equal to $\varepsilon_k - \varepsilon_i - 1/r_{ik}$. The transition that leads to an increase (or decrease) in the energy of an electron involves the absorption (or emission) of a phonon with an energy equal to the energy of the electron transition. The eigenvalue distribution $P(\lambda)$ of the "A matrix" controls the dynamics of the system, which was pushed marginally away from its local equilibrium state in this case.

The dynamics of the system can be categorized into four temporal zones, including the initial fast relaxation, slow relaxation at intermediate and long times, and the final decay to equilibrium. The initial fast relaxation is caused by the system relaxing through energy-lowering transitions between nearest-neighbor sites. At intermediate and long times, the slow relaxation is due to transitions, which result in an increase in the system's energy. The functional form of the eigenvalue distribution $P(\lambda)$ leads to different decay laws, and the system will eventually relax to equilibrium via exponential decay for times $t > 1/\lambda_{\min}$, where $\lambda_{\min}$ is the minimum eigenvalue of the "A matrix." We will discuss this in detail in the next section for screened and unscreened Coulomb interactions.

Slow dynamics are prevalent in systems having both interactions and disorder. Yet, distinguishing whether the dominant cause for slow dynamics lies in the interactions or in the

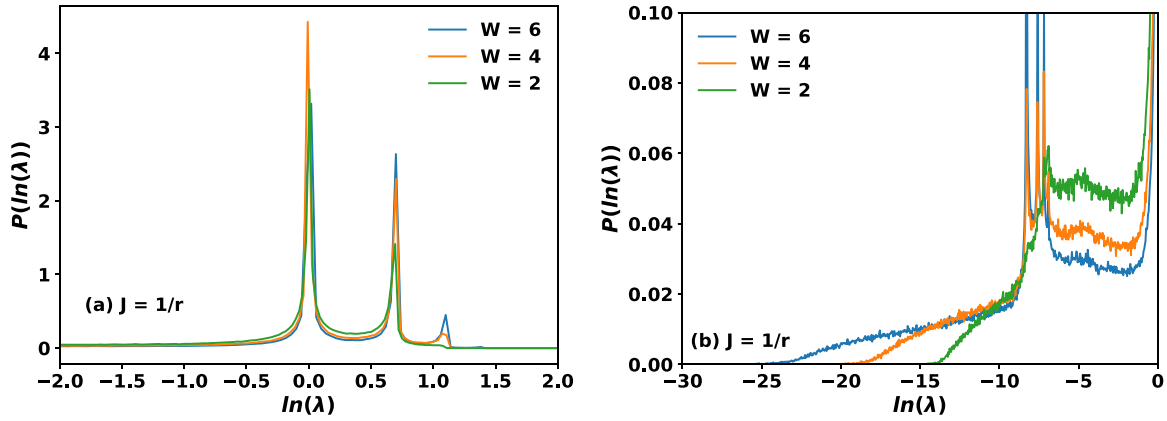

FIG. 2. Plot of the distribution of the $\ln(\lambda)$ of the dynamical matrix A obtained by solving Eq. (9) using Coulomb interactions [given in Eq. (2a)] at different disorders, (a) at short times and (b) intermediate and long times.

disorder may be difficult experimentally. Specifically, in the electron glass, changing the electron density changes both disorder and interaction strengths, making their independent study difficult. Nevertheless, numerical methods can be used to investigate the individual roles of disorder and interaction. To achieve this, three different scenarios are considered here: the unscreened Coulomb interaction case, the screened Coulomb interaction case, and the case where the ratio of disorder and interaction is kept constant to examine the relaxation dynamics.

1. Unscreened Coulomb interactions

In this section we study the relaxation dynamics of the system for the case of unscreened Coulomb interactions. In the first scenario, the interaction strength is kept constant while varying the disorder strength to determine the effect of the disorder on slow relaxation. The distribution $P(\ln(\lambda))$ of the eigenvalue λ of the "A matrix" is displayed in Fig. 2. The eigenvalues have been scaled by the factor $\exp(-1.0/\xi)$. The plot shows that $P(\ln(\lambda))$ displays peaks at high eigenvalues (initial times) corresponding to $\lambda = 1$ and 2. These peaks represent an electron relaxing to the nearest-neighbor site through an energy-lowering transition in the case of a single such available site ($\lambda = 1$) and two such available sites ($\lambda = 2$). At intermediate times, in the regime $\ln(\lambda) = -2$ to $\ln(\lambda) = -5$, the distribution $P(\ln(\lambda))$ is approximately parallel to the x axis as shown in Fig. 2(b). This implies that $P(\lambda) \approx c/\lambda$, and thus the fluctuations in the system decay by the logarithmic decay law, $\delta n(t) \sim \ln(t)$, at intermediate times for all disorders.

Subsequently, the relaxation process in the system occurs through electron transitions to the next-nearest-neighbor site, resulting in energy-lowering transitions. This phenomenon gives rise to peaks in the probability distribution at approximately $\ln\lambda \approx -8$ [see Fig. 2(b)]. Each peak corresponds to a specific number of available transition sites: one peak represents a single possible transition, while the other two peaks correspond to two and three available transition sites. This behavior is analogous to the peaks observed in Fig. 2(a) for nearest-neighbor transitions.

As time progresses, particularly at long timescales, the system undergoes relaxation to nearest or next-nearest-neighbor sites through transitions, which result in an increase in the system's energy within the range of $\lambda_{\min} < \lambda < e^{-10}$. This region can be further divided into two parts. Initially, there is a period of slow relaxation, $\ln(\lambda') < \ln(\lambda) < -10$, followed by a more pronounced decrease towards $\lambda_{\min}$. We observe that the system relaxes slowly until the time $t' = 1/\lambda'$, where the specific value of λ' depends on the disorder (as depicted in Fig. 3). Subsequently, the system exhibits exponential decay after the time $\tau = 1/\lambda_{\min}$. It is worth noting that these two distinct timescales, t' and τ, have also been observed experimentally [55].

To determine the slow relaxation law in the long time regime, $P(\lambda)$ vs $\ln(\lambda)$ is shown in Fig. 3. It is noted that the plot of $P(\lambda)$ against λ on a log-log scale is a straight line when λ is greater than λ', with an absolute value of the slope less than 1. This indicates that the relaxation follows a power-law decay [$\delta n(t) \sim t^{-\alpha}$]. The absolute value of the slope increases as W becomes larger, and for $W = 4$ and 6, it approaches 1, indicating that the behavior is close to logarithmic decay in these cases. The crossover from logarithmic decay to power-law behavior with $\alpha = 0.2$ with time has been observed in experiments [8], while in some experiments [9], only $\ln(t)$ behavior is observed.

For cases where $\lambda_{\min} t \ll 1$, the change in energy $\Delta E \propto \delta n(t)$ [62], and thus the energy decay will exhibit distinct behaviors depending on the form of the probability distribution $P(\lambda)$. Specifically, when $P(\lambda) = \lambda^{-1}$, the energy decay follows a logarithmic relationship, expressed as $\Delta E \propto \ln(t)$. On the other hand, when $P(\lambda) = \frac{1}{\lambda^{1-\alpha}}$, the energy decay is characterized by a power law, resulting in $\Delta E \propto t^{-\alpha}$. An assumption that holds some plausibility, though not entirely conclusive, is that the reduction in conductivity is directly proportional to the decrease in energy for timescales $t \ll \lambda_{\min}^{-1}$ [62].

We also observe [see Fig. 2(b)] that $P(\lambda)$ for the intermediate times decreases as the disorder increases. This implies that as the disorder increases, the probability of an electron finding a hole to be excited to with only a small energy gain at the nearest-neighbor site decreases. These electrons jump

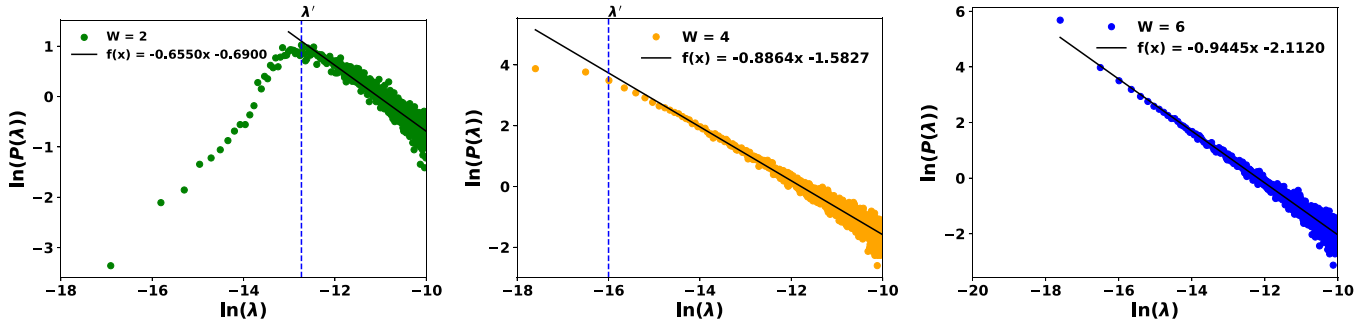

FIG. 3. The relaxation law governing the behavior of small eigenvalue distribution (in Coulomb interaction case) at long times, $P(\lambda) \propto c/\lambda^x$ (where x is provided by the slope of the straight line fit), are studied here for different disorders.

to higher energy holes (at long times) to relax as the disorder increases, leading to a decrease in the value of $\lambda_{\min}$. These effects can be explained by a decrease in the number of states around the Fermi level as the disorder increases. The number of holes in an energy range E above the Fermi level is proportional to E/W for energies inside the Coulomb gap and $1/W$ for sites outside the gap. Thus the probability of an electron finding a hole ($\Delta E > 0$ transitions) with energy E decreases as disorder increases. For transitions that result in an increase in the system's energy, $\lambda \propto e^{-\beta \Delta E}$, so $P(\lambda)$ at intermediate times and $\lambda_{\min}$ decrease with an increase in disorder. The system will eventually relax to a local equilibrium state via the exponential law $\delta n(t) = e^{-t/\tau}$. The value of $\tau = 1/\lambda_{\min}$ will increase with increasing disorder. The conundrum of whether the disorder or the Coulomb gap (due to long-range Coulomb interactions) is the primary cause of the slow relaxation arises from the fact that J/W is decreasing as W increases.

The finite-size analysis shows that the DOS at and around the Fermi level varies with the system's size. However, the impact on the eigenvalue distribution of the A matrix (P(λ)) and hence on dynamics is negligible. The details are discussed in Appendix.

2. *Screened Coulomb interactions*

In order to separate the effects of disorder and interaction, we now consider the case where the disorder is constant, but the interactions change as a result of the addition of a screening plate. The effect of disorder strength (W) and screening length (d) on the dynamics of the system is analyzed by keeping the disorder strength constant while screening the Coulomb interactions using the screened interaction specified in Eq. (2b). The behavior of $P(\lambda)$ is studied for various screening lengths and disorders, and the results are illustrated in Fig. 4.

At a fixed disorder level, it has been observed that the slope of $P(\ln(\lambda))$ versus $\ln(\lambda)$ increases as the screening parameter d decreases, specifically for intermediate and long timescales. Furthermore, the value of $\lambda_{\min}$, which represents the inverse of the longest relaxation time, also increases as d decreases. These findings suggest that the relaxation process becomes faster as the screening of Coulomb interaction increases. It is worth noting that the changes in the slope value and $\lambda_{\min}$ are relatively small when the disorder is sufficiently high, as depicted in Fig. 4(c).

The effect of screening on the relaxation dynamics is attributed to the smearing of the gap in the density of states (DOS) due to screening, as seen in Fig. 1(a). The screening leads to a sufficient number of electrons (holes) close to the Fermi level, allowing the system to relax to a low-energy state more effectively. The filling of the gap is found to be around 10%–25% for screening lengths corresponding to $d \geqslant 1.5$, as shown in Fig. 1(b). For these values of d, the difference in the slopes between screened and unscreened cases at $W = 4$ and 6 is small, and hence the system will decay via a nearly logarithmic law, similar to experimental observations [55] where Coulomb interactions were screened by a metallic plate, resulting in a 12%–23% filling of the Coulomb gap.

The effect of very strong screening ($d = 0.5$) on the dynamics is also studied. In Fig. 1(b) one observes that at $d = 0.5$, the gap is about 60% filled for all disorders. Upon comparison [see Figs. 5(a) and 4] one observes that $\lambda_{\min}$ increases substantially by a factor of approximately e^3 with respect to the unscreened case. This implies that the system will show slow relaxation for a much shorter period of time, which may not be observable experimentally. For the smallest disorder considered ($W = 2$), the system will show no logarithmic decay, and for $W = 4$ [see Fig. 5(b)], the system will decay via power law [$\delta n(t) = 1/t^{\alpha}$] for intermediate and long times with α values of 0.1136 and 0.3490, respectively. At high disorder ($W = 6$), as shown in Fig. 5(c), the system will decay via a nearly logarithmic law (with α values of 0.0555 and 0.1080 at intermediate and long times, respectively), showing that slow relaxation can happen without strong interaction effects consistent with the experimental findings [55].

To grasp the significance of the role of interactions on relaxation, we have analyzed the effect of doubling the interaction strength while keeping the disorder constant for the unscreened interaction case. Here we study a $W = 4$ case (see Fig. 6) in which the unscreened Coulomb interaction exhibits logarithmic decay at intermediate times. The relaxation time τ increases by a factor of approximately 10^3 (e^7) on doubling the interaction strength. This slowdown in the relaxation process is due to the doubling of the width of the Coulomb gap, leading to a significant decrease in DOS around the Fermi level. Experimentally [40], one has observed a rapid increase in τ as the width of the Coulomb gap increases. The Coulomb gap width is proportional to the strength of interaction, which is proportional to the square root of the carrier concentration. In experiments, increasing the carrier concentration also

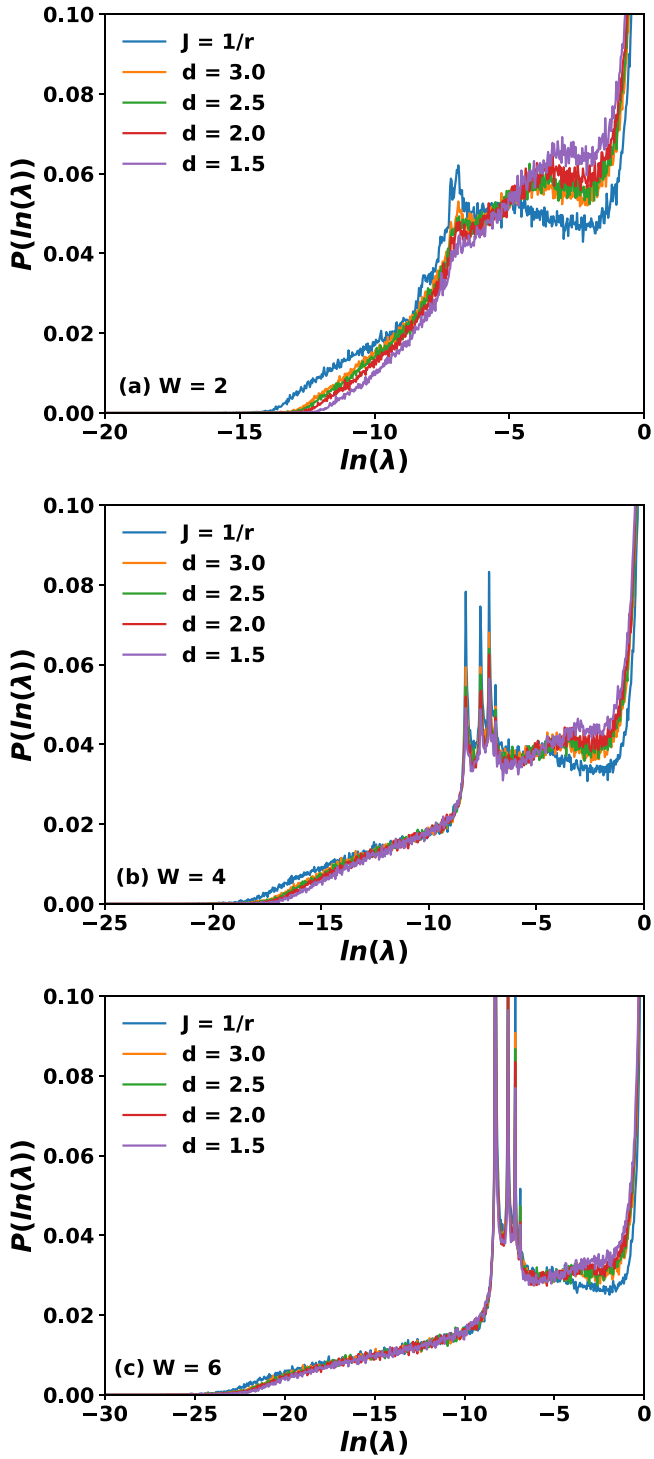

FIG. 4. Log-log plot of the distribution of the eigenvalues of the dynamical matrix A obtained by solving Eq. (9) using Coulomb interactions and screened interactions. (a)–(c) Represent the intermediate and long time behavior at $W = 2, 4,$ and 6, respectively. Here $J = 1/r$ corresponds to the Coulomb interaction case as defined in Eq. (2a), and $d = 1.5$ to $d = 3$ corresponds to the screened interaction case [see Eq. (2b)].

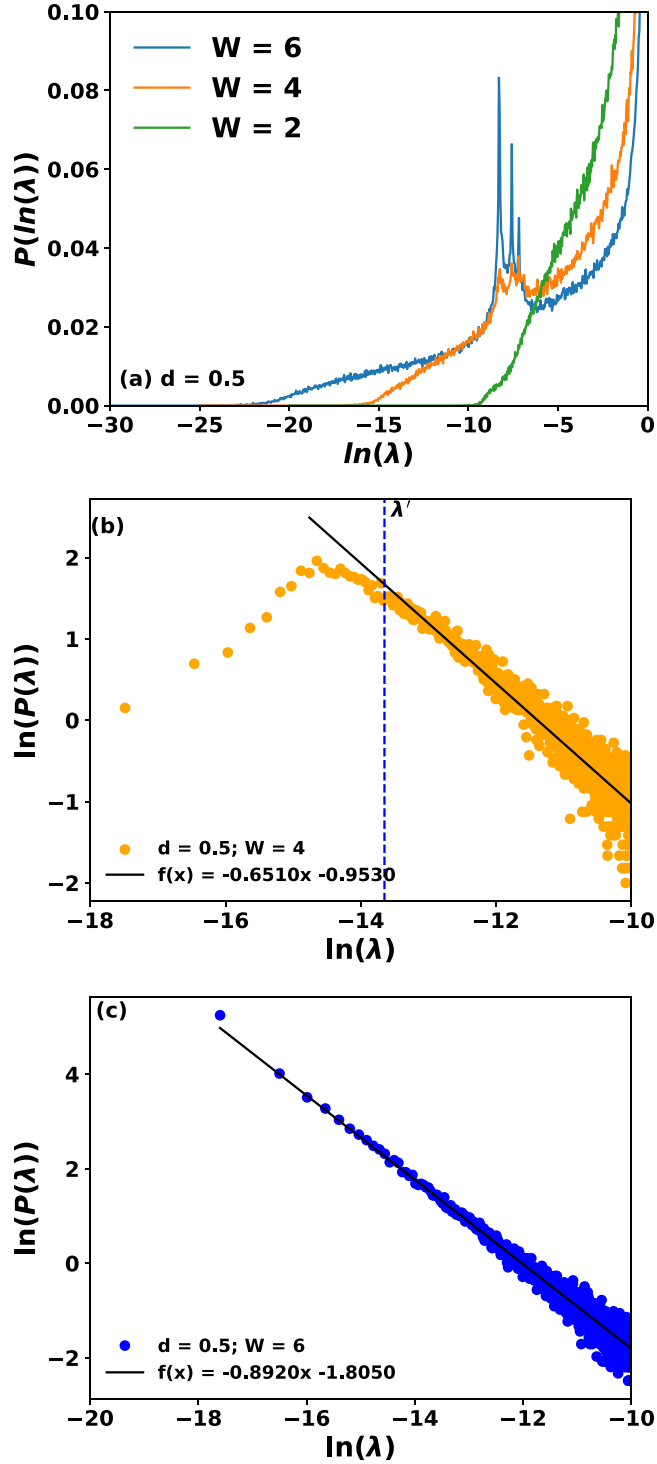

FIG. 5. (a) Log-log plot of the distribution of the eigenvalues of the dynamical matrix A obtained by solving Eq. (9) using screened interactions with $d = 0.5$ in Eq. (2b) at different disorders. The relaxation law governing the behavior of small eigenvalue distribution (in the screened interaction case) with $d = 0.5$ and $W = 4$. (c) The relaxation law governing the behavior of small eigenvalue distribution (in the screened interaction case) with $d = 0.5$ and $W = 6$.

leads to an increase in disorder [41], making it difficult to understand the role of interactions in the slow relaxation process when disorder and interaction strength are comparable. At later times, the power-law exponent α decreases significantly, and the decay becomes approximately logarithmic.

We will now examine the impact of doubling the interaction strength on relaxation dynamics under the condition

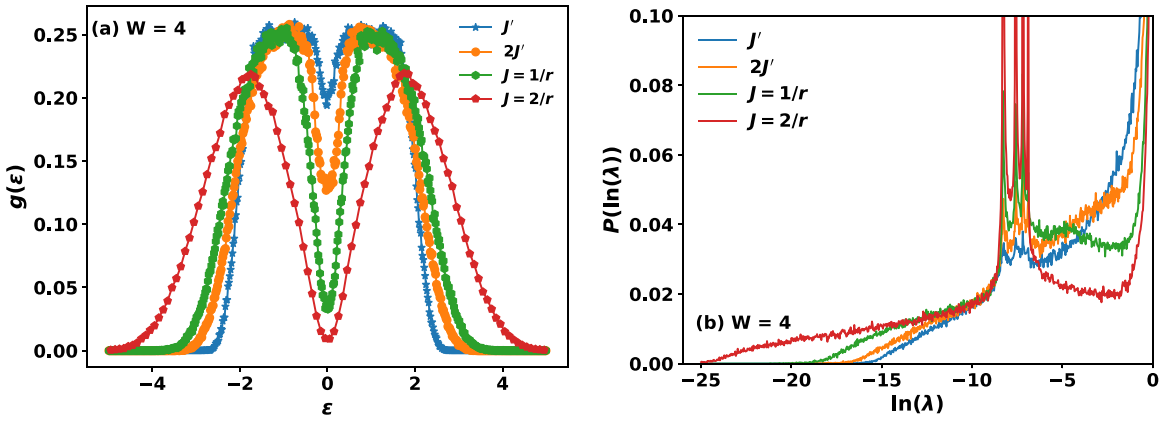

FIG. 6. (a) Histogram of the Hartree energies ε [obtained using Eq. (4)] for different interaction strengths at $W = 4$. (b) Log-log plot of the distribution of the eigenvalues of the dynamical matrix A obtained by solving Eq. (9). $J' = 1/r_{ik} - 1/\sqrt{r_{ik}^2 + 4d^2}$ and $2J' = 2/r_{ik} - 2/\sqrt{r_{ik}^2 + 4d^2}$ correspond to the screened interaction case where $d = 0.5$. $J = 1/r_{ik}$, and $J = 2/r_{ik}$ corresponds to the Coulomb interaction case.

of constant disorder, specifically focusing on the scenario of strong screening ($d = 0.5$). Comparison of $2J' = 2/r - 2/\sqrt{r^2 + 4d^2}$, $W = 4$ with $J' = 1/r - 1/\sqrt{r^2 + 4d^2}$, $W = 4$ where $d = 0.5$ [see Fig. 6(b)] shows that relaxation in both cases is similar. Thus in the case of strong screening, the interaction is now short range, and the degree of relaxation is mainly determined by the degree of disorder. Our results suggest that doubling the interaction without screening has a far more substantial effect on the dynamics than doubling the interaction in the strongly screened scenario. Another observation that is made from Fig. 6(a) is that the width of the Coulomb gap is roughly comparable for the two screened cases and the $J = 1/r$ case. The only notable variation is the Coulomb gap's dip. While the gap is well formed in the unscreened case, it is substantially filled in the two screened cases. As a result, the variation in τ values for these three scenarios is minimal, but logarithmic decay at intermediate times can only be seen for the unscreened Coulomb interaction. We provide a rough explanation for this behavior. The width of the Coulomb gap and the single-particle density of states (both depend upon the strength of interaction for constant disorder) affect the distribution's lowest eigenvalue. On the other hand, the depletion of the DOS at the Fermi level is responsible for the logarithmic time dependence observed at intermediate times for the unscreened Coulomb interaction.

3. Constant J/W ratio

Finally, in the third scenario both the disorder and interaction strength are increased while keeping their ratio constant. This scenario is expected to be similar to the experimental situation where the carrier concentration and disorder in a sample increase.

The results show that when both the disorder and interaction strength are doubled for the unscreened interaction case, the relaxation dramatically slows down. This is evident from the increase in τ, which is roughly 20 000 (e^{10}) times greater when $J = 2/r$ and $W = 4$ compared to when $J = 1/r$ and $W = 2$ [as shown in Fig. 7(b)]. The decrease in DOS around the Fermi level, as shown in Fig. 7(a), is attributed to both an increase in disorder and the widening of the Coulomb gap. Therefore for high disorder with unscreened interaction, the system decays according to the logarithmic law, but the relaxation time ($\tau = 1/\lambda_{\min}$) depends on the degree of disorder and interaction. The results for the strong screening scenario ($d = 0.5$), when the disorder and interaction are doubled, are also discussed [see Figs. 7(c) and 7(d)]. The lower value of DOS around the Fermi level and increase in the width of the distribution in the $W = 4$ case compared to the $W = 2$ case leads to slower relaxation as the disorder increases.

V. DISCUSSION

In summary, this study discusses the relaxation dynamics of a Coulomb glass model in relation to disorder and screening. The results show that the system relaxes via logarithmic decay at intermediate intervals, regardless of the degree of disorder, when unscreened Coulomb interactions are present. However, the system decays via power law [$\delta n(t) \sim t^{\alpha}$] at late times with a smaller exponent (α) as the disorder increases, and for strong disorders, the exponent can be almost zero, with logarithmic decay potentially visible in experiments. The relaxation is faster, and the deviation from logarithmic decay can be observed when the interactions are screened, and the density of states near the Fermi level plays a crucial role in explaining these findings. The system begins to relax gradually when there are few electronic states close to the Fermi level. The depletion of electronic states around the Fermi level is accelerated by increasing disorder and opening a Coulomb gap, which causes slower relaxation. The Coulomb gap is filled and narrowed due to the Coulomb interaction being screened, leading to faster relaxation. In the case of strong disorders with weak screening (where the gap is filled by 10%–25%), we observe that the relaxation behavior closely resembles that of the unscreened case. These findings are consistent with experimental observations where a metal plate was used to screen the Coulomb interaction, resulting in a filling of the gap by approximately 12%–23%. Our findings concerning strong screening within the high-disorder regime indicate that the relaxation dynamics are primarily governed by the disorder strength. In this scenario the time required to enter the exponential decay regime decreases compared to the

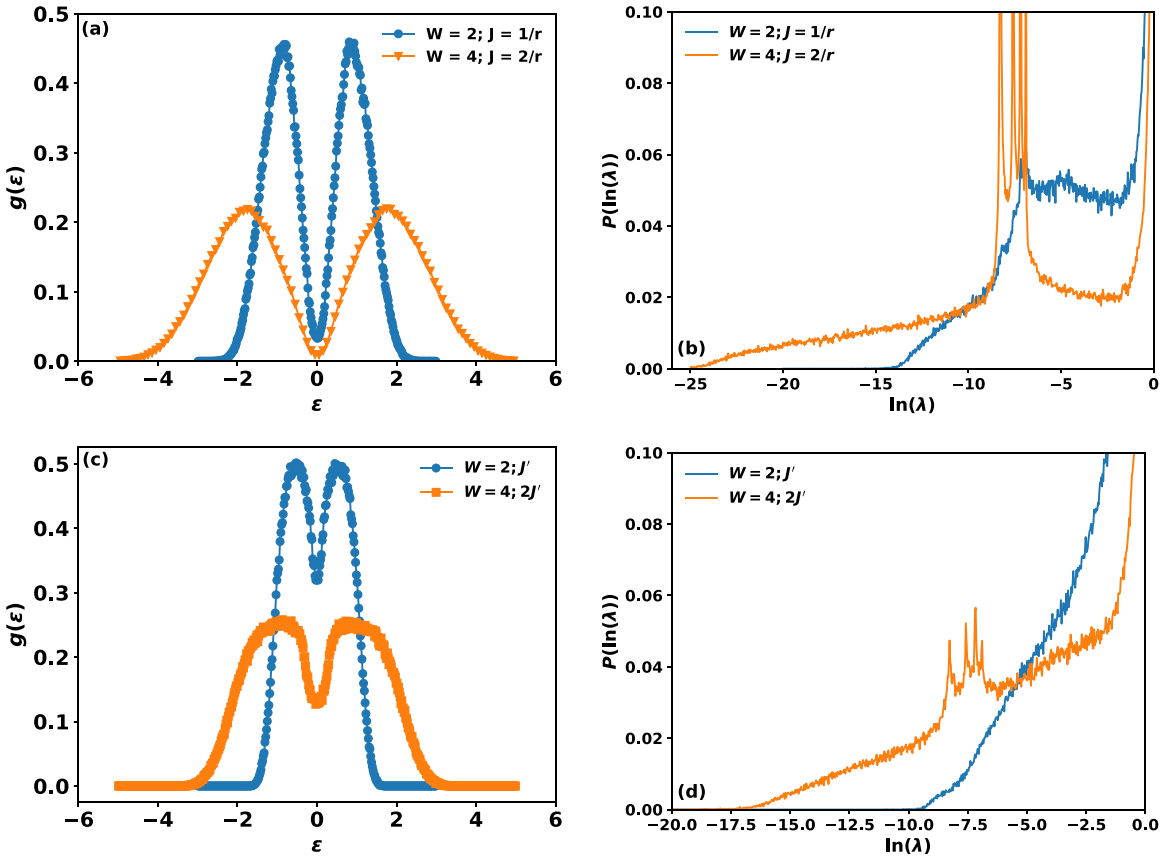

FIG. 7. (a)–(c) Histogram of the Hartree energies ε [obtained using Eq. (4)] for different disorder values and interaction strengths. (b)–(d) Log-log plot of the distribution of the eigenvalues of the dynamical matrix A obtained by solving Eq. (9). $J' = 1/r_{ik} - 1/\sqrt{r_{ik}^2 + 4d^2}$ and $2J' = 2/r_{ik} - 2/\sqrt{r_{ik}^2 + 4d^2}$ correspond to the screened interaction case where $d = 0.5$. $J = 1/r_{ik}$ and $J = 2/r_{ik}$ correspond to the Coulomb interaction case.

unscreened case, with the main determining factor being the disorder.

Furthermore, the study investigates the separate roles of disorder and interaction strength in determining the relaxation dynamics. In experiments on thin films, increasing the concentration (n) of sites in the material increases the interaction between electrons. When n increases, the interaction grows while the average distance between sites (r_{avg}) decreases. In a system with strong localization, the disorder strength will be of the order of Fermi energy, which rises with n. As a result, an increase in site density causes the ratio of interaction strength ($J = 1/r_{avg}$) to disorder strength (W) to decrease by $n^{1/2}$. In our model a rise in disorder causes a fall in the height and an increase in the width of the density of states, whereas a rise in interaction causes a rise in the width of the Coulomb gap and the DOS. Hence, both disorder and interaction strength contribute equally to sluggish relaxation when they are of similar strength. The relaxation time (τ), after which fluctuations follow the exponential decay law towards equilibrium, is another crucial parameter in experiments. In agreement with experiments, our results show that the τ increases very fast as the strength of the interaction is increased, keeping the disorder strength constant. The increase in τ is even more when both disorder and interaction strength

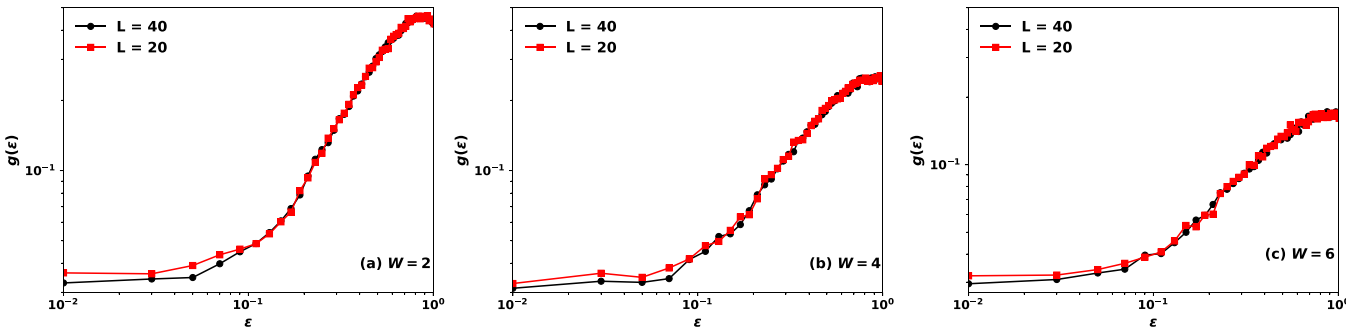

FIG. 8. Comparing the single-particle density of states on a logarithmic scale for system sizes $L = 40$ and $L = 20$ at disorder W in the Coulomb interactions case.

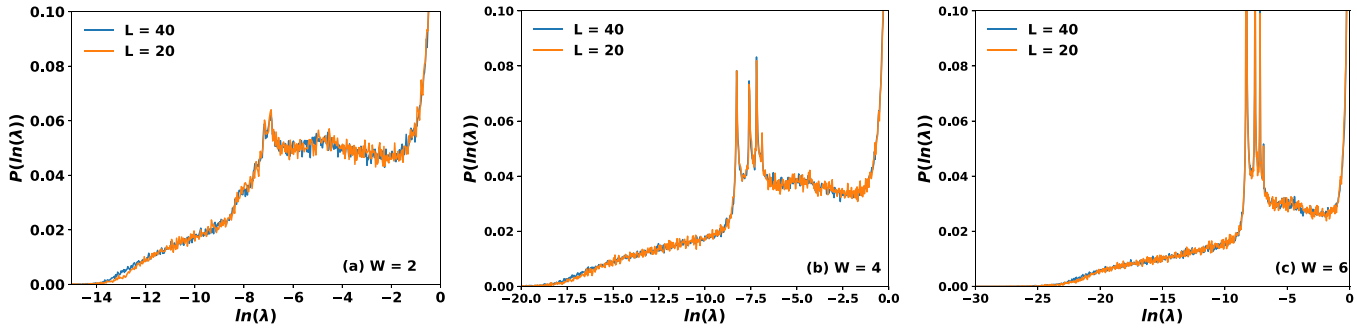

FIG. 9. Comparing the distribution of the eigenvalues of the dynamical matrix A on a logarithmic scale for system sizes of $L = 40$ and $L = 20$ at disorder W in the Coulomb interactions case.

increase, which was also observed experimentally. According to our data, τ decreases quickly as system disorder decreases, but interaction strength stays the same. This could explain why slow relaxation is not seen in semiconductors with light doping.

Our work is able to qualitatively explain the role of interaction and disorder strength as well as the screening of Coulomb interaction in the slow relaxation of the CG system. However, to reach experimental timescales of 10^3 s or higher can be achieved by a Monte Carlo simulation [67,68] tailored to probe long timescales.

Overall, our results suggest that the intermediate and long-time dynamics are dictated by the DOS near the Fermi energy and far from the Fermi energy, respectively. Thus, and since disorder dictates a pseudogap in the DOS, we find that at large disorders, the decay is logarithmic and slows down with increased disorder. And also, interactions decrease the DOS near the Fermi energy and cause slower dynamics.

ACKNOWLEDGMENTS

V.M. acknowledges the funding from SERB, Department of Science and Technology, Government of India, under Research Grant No. CRG/2022/004029. M.S. acknowledges support from the Israel Science Foundation (Grant No. 2300/19). P.B. acknowledges Ben-Gurion University of the Negev for access to their HPC resources. Illuminating discussions with Z. Ovadyahu are gratefully acknowledged.

APPENDIX: FINITE-SIZE EFFECT

We have examined the impact of system size on the density of states (DOS) and the distribution of eigenvalues of the A matrix (P(λ)) within the context of unscreened Coulomb interactions. Figure 8 illustrates the finite-size effects on the density of states near the Fermi level for disorder strengths of $W = 2, 4$, and 6. Additionally, Fig. 9 presents the finite-size behavior of the probability distribution $P(\lambda)$ of eigenvalues (λ) of the dynamical matrix (A matrix) under different disorder strengths for the unscreened Coulomb interactions case. It is observed that when $|\varepsilon| \leqslant 0.1$, there are variations in the density of states with respect to the system size. However, as seen from Fig. 9, these variations have a negligible impact on $P(\lambda)$ and hence on the relaxation dynamics.

[1] P. Bhandari, V. Malik, D. Kumar, and M. Schechter, Relaxation dynamics of the three-dimensional Coulomb glass model, Phys. Rev. E **103**, 032150 (2021).

[2] A. B. Kolton, D. R. Grempel, and D. Domínguez, Heterogeneous dynamics of the three-dimensional Coulomb glass out of equilibrium, Phys. Rev. B **71**, 024206 (2005).

[3] M. Kirkengen and J. Bergli, Slow relaxation and equilibrium dynamics in a two-dimensional Coulomb glass: Demonstration of stretched exponential energy correlations, Phys. Rev. B **79**, 075205 (2009).

[4] A. L. Burin, B. I. Shklovskii, V. I. Kozub, Y. M. Galperin, and V. Vinokur, Many electron theory of 1/f noise in hopping conductivity, Phys. Rev. B **74**, 075205 (2006).

[5] L. F. Cugliandolo and J. Kurchan, Analytical Solution of the Off-Equilibrium Dynamics of a Long-Range Spin-Glass Model, Phys. Rev. Lett. **71**, 173 (1993).

[6] L. F. Cugliandolo and J. Kurchan, On the out-of-equilibrium relaxation of the Sherrington-Kirkpatrick model, J. Phys. A: Math. Gen. **27**, 5749 (1994).

[7] A. Vaknin, Z. Ovadyahu, and M. Pollak, Aging Effects in an Anderson Insulator, Phys. Rev. Lett. **84**, 3402 (2000).

[8] A. Vaknin, Z. Ovadyahu, and M. Pollak, Heuristic model for slow relaxation of excess conductance in electron glasses, Phys. Rev. B **61**, 6692 (2000).

[9] A. Vaknin, Z. Ovadyahu, and M. Pollak, Nonequilibrium field effect and memory in the electron glass, Phys. Rev. B **65**, 134208 (2002).

[10] V. Orlyanchik and Z. Ovadyahu, Stress Aging in the Electron Glass, Phys. Rev. Lett. **92**, 066801 (2004).

[11] V. I. Kozub, Y. M. Galperin, V. Vinokur, and A. L. Burin, Memory effects in transport through a hopping insulator: Understanding two-dip experiments, Phys. Rev. B **78**, 132201 (2008).

[12] M. Ben-Chorin, Z. Ovadyahu, and M. Pollak, Nonequilibrium transport and slow relaxation in hopping conductivity, Phys. Rev. B **48**, 15025 (1993).

[13] G. Martinez-Arizala, D. E. Grupp, C. Christiansen, A. M. Mack, N. Markovic, Y. Seguchi, and A. M. Goldman,

Anomalous Field Effect in Ultrathin Films of Metals near the Superconductor-Insulator Transition, Phys. Rev. Lett. **78**, 1130 (1997).
[14] G. Martinez-Arizala, C. Christiansen, D. E. Grupp, N. Marković, A. M. Mack, and A. M. Goldman, Coulomb-glass-like behavior of ultrathin films of metals, Phys. Rev. B **57**, R670(R) (1998).
[15] J. H. Davies, P. A. Lee, and T. M. Rice, Electron Glass, Phys. Rev. Lett. **49**, 758 (1982).
[16] M. Grunewald, B. Pohlmann, L. Schweitzer, and D. Wurtz, Mean field approach to the electron glass, J. Phys. C **15**, L1153 (1982).
[17] M. Pollak and M. Ortuno, Coulomb interactions in Anderson localized disordered systems, Solar Energy Mater. **8**, 81 (1982).
[18] M. Pollak, Non-ergodic behaviour of anderson insulators with and without Coulomb interactions, Philos. Mag. B **50**, 265 (1984).
[19] E. R. Grannan and C. C. Yu, Grannan and Yu Reply, Phys. Rev. Lett. **73**, 2934 (1994).
[20] M. Müller and L. B. Ioffe, Glass Transition and the Coulomb Gap in Electron Glasses, Phys. Rev. Lett. **93**, 256403 (2004).
[21] A. A. Pastor and V. Dobrosavljević, Melting of the Electron Glass, Phys. Rev. Lett. **83**, 4642 (1999).
[22] S. Pankov and V. Dobrosavljević, Nonlinear Screening Theory of the Coulomb Glass, Phys. Rev. Lett. **94**, 046402 (2005).
[23] M. Müller and S. Pankov, Mean-field theory for the three-dimensional Coulomb glass, Phys. Rev. B **75**, 144201 (2007).
[24] A. Bray and M. Moore, Spin glasses: The hole story, J. Phys. C **15**, 2417 (1982).
[25] A. Amir, Y. Oreg, and Y. Imry, Slow Relaxations and Aging in the Electron Glass, Phys. Rev. Lett. **103**, 126403 (2009).
[26] A. Amir, Y. Oreg, and Y. Imry, Mean-field model for electron-glass dynamics, Phys. Rev. B **77**, 165207 (2008).
[27] A. L. Éfros and B. I. Shklovskii, Coulomb gap and low temperature conductivity of disordered systems, J. Phys. C **8**, L49 (1975).
[28] B. I. Shklovskii and A. L. Efros, *Electronic Properties of Doped Semiconductors* (Springer Science & Business Media, New York, 2013), Vol. 45.
[29] S. Baranovskii, A. Efros, B. Gelmont, and B. Shklovskii, Coulomb gap in disordered systems: Computer simulation, J. Phys. C **12**, 1023 (1979).
[30] J. H. Davies, P. A. Lee, and T. M. Rice, Properties of the electron glass, Phys. Rev. B **29**, 4260 (1984).
[31] A. Möbius, M. Richter, and B. Drittler, Coulomb gap in two- and three-dimensional systems: Simulation results for large samples, Phys. Rev. B **45**, 11568 (1992).
[32] A. Glatz, V. M. Vinokur, J. Bergli, M. Kirkengen, and Y. M. Galperin, The Coulomb gap and low energy statistics for Coulomb glasses, J. Stat. Mech.: Theory Exp. (2008) P06006.
[33] P. Bhandari, V. Malik, and S. R. Ahmad, Critical behavior of the two-dimensional Coulomb glass at zero temperature, Phys. Rev. B **95**, 184203 (2017).
[34] P. Bhandari and V. Malik, Effect of increasing disorder on domains of the 2D Coulomb glass, J. Phys.: Condens. Matter **29**, 485402 (2017).
[35] M. Goethe and M. Palassini, Phase Diagram, Correlation Gap, and Critical Properties of the Coulomb Glass, Phys. Rev. Lett. **103**, 045702 (2009).
[36] B. Surer, H. G. Katzgraber, G. T. Zimanyi, B. A. Allgood, and G. Blatter, Density of States and Critical Behavior of the Coulomb Glass, Phys. Rev. Lett. **102**, 067205 (2009).
[37] A. Möbius and M. Richter, Comment on "Density of States and Critical Behavior of the Coulomb Glassm," Phys. Rev. Lett. **105**, 039701 (2010).
[38] M. Sarvestani, M. Schreiber, and T. Vojta, Coulomb gap at finite temperatures, Phys. Rev. B **52**, R3820(R) (1995).
[39] Z. Ovadyahu and M. Pollak, Disorder and Magnetic Field Dependence of Slow Electronic Relaxation, Phys. Rev. Lett. **79**, 459 (1997).
[40] A. Vaknin, Z. Ovadyahu, and M. Pollak, Evidence for Interactions in Nonergodic Electronic Transport, Phys. Rev. Lett. **81**, 669 (1998).
[41] Z. Ovadyahu, Slow dynamics of electron glasses: The role of disorder, Phys. Rev. B **95**, 134203 (2017).
[42] Z. Ovadyahu, Transition to exponential relaxation in weakly disordered electron glasses, Phys. Rev. B **97**, 214201 (2018).
[43] V. Orlyanchik and Z. Ovadyahu, Electron glass in samples approaching the mesoscopic regime, Phys. Rev. B **75**, 174205 (2007).
[44] J. Delahaye, T. Grenet, C. A. Marrache-Kikuchi, V. Humbert, L. Bergé, and L. Dumoulin, Electron glass effects in amorphous NbSi films, SciPost Phys. **8**, 056 (2020).
[45] M. Pollak and Z. Ovadyahu, A model for the electron glass, Phys. Status Solidi C **3**, 283 (2006).
[46] C. Sagui, A. M. Somoza, and R. C. Desai, Spinodal decomposition in an order-disorder phase transition with elastic fields, Phys. Rev. E **50**, 4865 (1994).
[47] A. Maheshwari and A. J. Ardell, Morphological Evolution of Coherent Misfitting Precipitates in Anisotropic Elastic Media, Phys. Rev. Lett. **70**, 2305 (1993).
[48] Z. Ovadyahu and M. Pollak, History-dependent relaxation and the energy scale of correlation in the electron glass, Phys. Rev. B **68**, 184204 (2003).
[49] T. Grenet, Symmetrical field effect and slow electron relaxation in granular aluminium, Eur. Phys. J. B **32**, 275 (2003).
[50] Z. Ovadyahu, Infrared-Induced Sluggish Dynamics in the GeSbTe Electron Glass, Phys. Rev. Lett. **115**, 046601 (2015).
[51] Z. Ovadyahu, Conductance Relaxation in the Electron Glass: Microwave Versus Infrared Response, Phys. Rev. Lett. **102**, 206601 (2009).
[52] C. C. Yu, Time-Dependent Development of the Coulomb Gap, Phys. Rev. Lett. **82**, 4074 (1999).
[53] V. Malik and D. Kumar, Formation of the Coulomb gap in a Coulomb glass, Phys. Rev. B **69**, 153103 (2004).
[54] E. Lebanon and M. Müller, Memory effect in electron glasses: Theoretical analysis via a percolation approach, Phys. Rev. B **72**, 174202 (2005).
[55] Z. Ovadyahu, Screening the Coulomb interaction and thermalization of Anderson insulators, Phys. Rev. B **99**, 184201 (2019).
[56] O. Asban, A. Burin, A. Shnirman, and M. Schechter, Polaronic effect of a metal layer on variable range hopping, Phys. Rev. B **103**, 045129 (2021).
[57] A. Efros, Coulomb gap in disordered systems, J. Phys. C **9**, 2021 (1976).
[58] A. L. Efros, B. Skinner, and B. I. Shklovskii, Coulomb gap in the one-particle density of states in three-dimensional systems with localized electrons, Phys. Rev. B **84**, 064204 (2011).

[59] A. Mobius, P. Karmann, and M. Schreiber, Coulomb gap revisited–a renormalisation approach, J. Phys.: Conf. Ser. **150**, 022057 (2009).

[60] F. G. Pikus and A. L. Efros, Critical Behavior of Density of States in Disordered System with Localized Electrons, Phys. Rev. Lett. **73**, 3014 (1994).

[61] F. G. Pikus and A. L. Efros, Coulomb gap in a two-dimensional electron gas with a close metallic electrode, Phys. Rev. B **51**, 16871 (1995).

[62] M. Pollak, M. Ortuño, and A. Frydman, *The Electron Glass* (Cambridge University Press, Cambridge, England, 2013).

[63] E. Bardalen, J. Bergli, and Y. M. Galperin, Coulomb glasses: A comparison between mean field and Monte Carlo results, Phys. Rev. B **85**, 155206 (2012).

[64] P. Bhandari, V. Malik, and M. Schechter, Variable range hopping in a nonequilibrium steady state, Phys. Rev. B **108**, 024203 (2023).

[65] O. Asban, A. Amir, Y. Imry, and M. Schechter, Effect of interactions and disorder on the relaxation of two-level systems in amorphous solids, Phys. Rev. B **95**, 144207 (2017).

[66] S. Puri, Kinetics of phase transitions, in *Kinetics of Phase Transitions* (CRC Press, Boca Raton, FL, 2009), pp. 13–74.

[67] A. M. Somoza, M. Ortuño, M. Caravaca, and M. Pollak, Effective Temperature in Relaxation of Coulomb Glasses, Phys. Rev. Lett. **101**, 056601 (2008).

[68] A. Pérez-Garrido, M. Ortuno, A. Díaz-Sánchez, and E. Cuevas, Numerical study of relaxation in electron glasses, Phys. Rev. B **59**, 5328 (1999).